

Article

Ablation of Copper Metal Films by Femtosecond Laser Multipulse Irradiation

Ahmed Abdelmalek ^{1,*}, Zeyneb Bedrane ¹ , El-Hachemi Amara ², Belén Sotillo ³,
Vibhav Bharadwaj ³, Roberta Ramponi ³  and Shane M. Eaton ³

¹ Physics Department, Theoretical Physics Laboratory, Tlemcen University, Tlemcen 13000, Algeria; zeyneb_bedrane@yahoo.fr

² Centre de Développement des Technologies Avancées, CDTA, PO. Box 17 Baba-Hassen, Algiers 16303, Algeria; amara@cda.dz

³ IFN-CNR and Dipartimento di Fisica, Politecnico di Milano, 20133 Milano, Italy; bsotillo@gmail.com (B.S.); vibhavbharadwaj@gmail.com (V.B.); roberta.ramponi@polimi.it (R.R.); shane.eaton@gmail.com (S.M.E.)

* Correspondence: ahmed7abdelmalek13@gmail.com; Tel.: +213-550-714-262

Received: 30 August 2018; Accepted: 12 September 2018; Published: 5 October 2018



Abstract: Ablation of copper using multipulse femtosecond laser irradiation with an 800 nm wavelength and 120-fs pulse duration is investigated theoretically. A two-temperature model, which includes dynamic optical and thermal-physical properties, is considered. The numerical results of the material thermal response obtained by varying the pulse number, the separation times between pulses and laser fluences are presented. Our results show that the increasing of pulse number with a separation time less than the thermal relaxation time can dramatically enhance the lattice temperature without a noticeable increase in ablation depth. Therefore, we suggest that the vaporization rate can be augmented in comparison to the melting rate during the same single-phase explosion at the same total fluence where a fast heat accumulation effect plays an important role for cleaner ablation during micromachining.

Keywords: femtosecond laser; metal ablation; two-temperature model; thermal accumulation effect

1. Introduction

As the number of applications targeted at ultrafast laser processing increases, there is even greater need to grasp the physical phenomena involved in the laser-material interaction, in order to achieve better control and quality of the patterned features. The drilling or micromachining by femtosecond laser garners much attention in scientific research because of its ablation precision compared to nanosecond or longer laser pulse durations [1–5]. In general, the physical mechanisms of metal ablation by femtosecond laser are still under study, where it has been observed that there are two different ablation phases during the transition from low to high fluence [3], gentle and strong ablation [6], respectively. Indeed, to produce ablation with high precision, one must apply the lowest above-threshold fluence possible to ensure that the damage of the material is minimized [2]. However, sometimes, this condition is not so practical from an industrial point of view.

Several models have been proposed to understand ultrashort laser pulse ablation. Gamaly et al. [7] suggested that matter is ejected by Coulomb Explosion (CE) after the creation of an intense electric field due to charge separation; however, the model presents an inconvenience concerning the nature of the solid material, with Stoian et al. [8] later clarifying that this type of explosion is dominant only in the case of dielectrics. Jian et al. [9] applied a classical approach where they assumed that the energy transfer to the lattice occurs by electron-ion collisions instead of electron-phonon collisions. Cheng et al. [10] proposed that phase explosion is the mechanism

responsible for matter removal using Molecular Dynamics simulations (MD), also supported by the most widely-used Two Temperature Model (TTM) [11,12].

If phase explosion is the dominant mechanism for ablation of a metal film irradiated by femtosecond laser pulses, the melted matter can be superheated without boiling, because the relaxation time is too short, such that a heterogeneous nucleation is produced. Consequently, when the temperature of the superheated liquids approaches the spinode (the limit of metastable phase heating [10]), i.e., when the temperature is close to the critical temperature of thermodynamic equilibrium T_c , the liquid's tension rapidly drops to zero. Therefore, the homogeneous bubble nucleation occurs at an extremely high rate. The superheated liquid relaxes via the thermal explosion process, and the ejected matter is a mixture of vapor and liquid droplets [10,13,14].

Ren et al. [15] simulated the ablation of a metallic target using bursts of 120-fs laser pulses. They found that under the same total fluence, a laser burst with a pulse separation time of 50 ps or longer than thermal relaxation time could significantly boost the ablation rate compared to the single pulse. We believe this effect may be due to a series of phase explosion processes during the irradiation with different rates of superheated liquid, because the pulse separation time is longer than the electron-phonon relaxation time.

Huang et al. [16] observed that the ablation of gold thin film irradiated by multiple femtosecond laser pulses, separated by a time of 280 ps, causes a peak in the temperature of electrons and the lattice. The lattice temperature after the arrival of a subsequent pulse is much higher, due to the residual heat energy already deposited by the first pulse. This enhancement in lattice temperature is due to thermal accumulation effect, because the time between pulses is shorter than the diffusion time of the thermal wave [17].

Ancona et al. [18] showed that this heat accumulation induced by high repetition rate causes a rapid increase in the mean temperature of the irradiated region, as subsequent pulses interact with a pre-heated volume. Therefore, less energy is necessary for ablation, and drilling efficiency increases significantly.

Extremely high repetition rate (GHz) bursts have been proposed by Kerse et al. [19] for efficient ablation enabled by ablation cooling. This work was supported by theoretical simulations by Povarnitsyn et al. [20].

In this regard, we propose a Fast Thermal Accumulation Effect (FTAE) induced by bursts with a short interpulse separation time lower than the thermal relaxation time, which can dramatically enhance the lattice temperature within the irradiated focal volume, thus reducing the energy dissipation into deeper material. Therefore, there will be an overheating of the same superheated liquid induced by the first pulse, which implies that the evaporation rate can be enhanced during the same single-phase explosion. As a result, a very high drilling efficiency can be obtained by this technique at high total fluence.

We study the thermal response of a copper metal film irradiated by a single and a burst of femtosecond laser pulses using the TTM with dynamic thermal and optical properties. The simulated ablation depths with single-pulse femtosecond laser irradiation are compared to the existing experimental data. The numerical results of thermal response and ablation depth generated by the multipulse femtosecond laser irradiation, having different pulse numbers and separation time, are presented and discussed.

2. Theoretical Background

2.1. Two Temperature Model

We have chosen a metal target (copper foil) of thickness $d = 3 \mu\text{m}$ and at initial temperature $T_0 = 300 \text{ K}$ irradiated by ultrashort laser pulses of fluence F on the front surface ($z = 0$).

The laser pulse is Gaussian in time with a Full Width at Half Maximum (FWHM) t_p of 120 fs with a central wavelength of 800 nm. The evolution of electron-lattice temperature can be described by the TTM [11,21]:

$$C_e(T_e) \frac{\partial T_e}{\partial t} = \frac{\partial}{\partial z} (k_e \frac{\partial T_e}{\partial z}) - G(T_e - T_l) + S(z, t) \tag{1}$$

$$C_l \frac{\partial T_l}{\partial t} = G(T_e - T_l) \tag{2}$$

C is the heat capacity; k is thermal conductivity, where e and l denote electron and lattice, respectively. G is the electron-phonon coupling factor. z is the direction perpendicular to the target surface (the model is considered in one dimension implying that the temperature is calculated just in the center of the focal volume), and t is the time.

The heat density S can be expressed for a single pulse as [21]:

$$S(z, t) = 0.94 \frac{1 - R}{t_p(\delta + \delta_b)(1 - e^{-d/(\delta + \delta_b)})} F \cdot \exp\left[\frac{-z}{(\delta + \delta_b)} - 2.77\left(\frac{t}{t_p}\right)^2\right] \tag{3}$$

We generalize this expression for the case of a multipulse per burst as follows:

$$S(z, t) = \sum_{i=1}^N 0.94 \frac{1 - R}{t_p(\delta + \delta_b)(1 - e^{-d/(\delta + \delta_b)})} F \cdot \exp\left[\frac{-z}{(\delta + \delta_b)} - 2.77\left(\frac{t - (i - 1)t_{sep}}{t_p}\right)^2\right] \tag{4}$$

where N is the number of pulses per burst, t_{sep} is the separation time between pulses, $\delta = 1/\alpha$ is the absorption depth, α is the absorption coefficient and R the reflectivity. δ_b is the ballistic range, where δ_b can be calculated as $\delta_b = v_e t_b$, v_e being the electron velocity calculated by: $v_e = \sqrt{\frac{2k_B T_e}{m_e^*}}$, where k_B is the Boltzmann constant, and $m_e^* = 1.41m_e$ is the effective mass of an electron [22], with $m_e = 9.1 \times 10^{-31}$ kg. $t_b = 24.7$ fs is the Drude relaxation time given by the relationship $t_b = \frac{m_e \sigma}{n_e e^2}$ where $\sigma = 5.88 \times 10^7 \text{ohmm}^{-1}$ is the electrical conductivity and $n_e = 8.45 \times 10^{28} \text{m}^{-3}$ is electrons' density [23]. The ballistic range value has an important impact in the simulations since it provides the ballistic transport of energy by the hot electrons. More details of its role can be found in [21]. Note that electrical conductivity also depends on the temperature, but we take it as constant to simplify the simulation and reduce the computation time.

2.2. Dynamic Thermal Properties

Here, the dynamical thermal parameters of copper are described briefly. In this work, we take the electron heat capacity as being proportional to electron temperature $C_e = \gamma T_e$, where $\gamma = 97 \text{Jm}^{-3}\text{K}^{-2}$ is the material constant and $C_l = 3.46 \times 10^6 \text{Jm}^{-3}\text{K}$ is the lattice heat capacity [14].

The heat diffusion of the electron subsystem is much faster than that of the lattice, where in well-conducting metals such as copper, the lattice component of the thermal conductivity comprises only about 1% of the total, the rest being due to the electrons [21]. Therefore, thermal conductivity of the lattice can be neglected, as it is very small in comparison with electron thermal conductivity, where the electron thermal conductivity k_e value was calculated using the general solution provided by Animisov et al. [24]:

$$k_e = \chi \frac{(\Phi_e^2 + 0.16)^{5/4} (\Phi_e^2 + 0.44) \Phi_e}{(\Phi_e^2 + 0.092)^{1/2} (\Phi_e^2 + \beta \Phi_l)} \tag{5}$$

where $\Phi_e = \frac{T_e}{T_F}$, $T_F = 8.12 \times 10^4 \text{K}$ is the Fermi temperature [23] and $\chi = 377 \text{Wm}^{-1}\text{K}^{-1}$ and $\beta = 0.139$ are constants for copper [11].

Electron-phonon coupling factor G , related to the rate of the energy exchange between the electrons and the lattice, can be expressed as [25]:

$$G = G_0 \left[\frac{A_e}{B_l} (T_e + T_l) + 1 \right] \tag{6}$$

where $G_0 = 0.5551 \times 10^{17} \text{ Wm}^{-3}\text{K}^{-1}$ is the coupling factor at room temperature and A_e and B_l represent the material constants for electron relaxation time, being $1.75 \times 10^7 \text{ K}^{-2}\text{s}^{-1}$ and $1.98 \times 10^{11} \text{ K}^{-1}\text{s}^{-1}$, respectively [11,14].

2.3. Dynamic Optical Properties

Using the simple Drude model, we study the evolution of the reflectivity and absorption coefficient of the copper surface during the irradiation by fs laser pulses.

The dielectric function of copper is [26]:

$$\varepsilon = \varepsilon_\infty - \frac{\omega_p^2}{\omega(\omega + \frac{i}{\tau_D})} = \varepsilon_\infty - \frac{\omega_p^2 \tau_D^2}{1 + \omega_p^2 \tau_D^2} + i \frac{\omega_p^2 \tau_D}{\omega(1 + \omega_p^2 \tau_D^2)} = \varepsilon_1 + i\varepsilon_2 \tag{7}$$

where τ_D is the relaxation time of the electrons in the metal and ω_p is the plasma frequency. $\varepsilon_\infty = 9.428$ is the dielectric constant. τ_D can be expressed as [15]:

$$\tau_D = (A_e T_e^2 + 1.41 \vartheta_{e,p})^{-1} \tag{8}$$

where the expression of the electron-phonon collision rate $\vartheta_{e,p}$ can be found in detail in [27].

Therefore, the refractive index n_r and extinction coefficient n_i can be written as:

$$n_r = \sqrt{\frac{\varepsilon_1 + \sqrt{\varepsilon_1^2 + \varepsilon_2^2}}{2}} \tag{9}$$

$$n_i = \sqrt{\frac{-\varepsilon_1 + \sqrt{\varepsilon_1^2 + \varepsilon_2^2}}{2}} \tag{10}$$

The absorption coefficient α and normal-incidence reflectivity R can be determined from the Fresnel function [28]. Neglecting the strongly spatial inhomogeneity due to material rarefaction and ionization, we assume these formulas (Equations (11) and (12)) are valid at multipulse laser ablation of high laser fluence with picosecond delay between pulses:

$$R = \frac{(n_r - 1)^2 + n_i^2}{(n_r + 1)^2 + n_i^2} \tag{11}$$

$$\alpha = \frac{4\pi}{\lambda} n_i \tag{12}$$

where λ is the laser wavelength. This dynamic TTM was simulated using MATLAB software by the finite differential method.

3. Results and Discussion

The numerical simulations were carried out for copper films irradiated by single and multipulse femtosecond laser irradiation with varying fluence, number of pulses and separation times. The choice of copper as a target and these specific parameters of the laser was to be able to compare our results with those available in the literature [15,16,29].

Figure 1 shows the calculated reflectivity R and absorption coefficient α , from Equations (11) and (12), as a function of temperature at an 800-nm wavelength. This figure indicates that R and α decrease dramatically with temperature. The decrease in R causes the target to absorb more laser energy, while the decrease in α changes the distribution of the laser's heat density S inside the target. It is obvious that these properties influence the amount of laser energy deposition and distribution during the irradiation and then affect the thermal response (ablation rate) of the material. This is why the optical dynamics must be taken into account during the simulation. Yang et al. [14], Chowdhury et al. [21] and Kotsedi et al. [30] considered R and α as constants, which may be valid only at low temperatures.

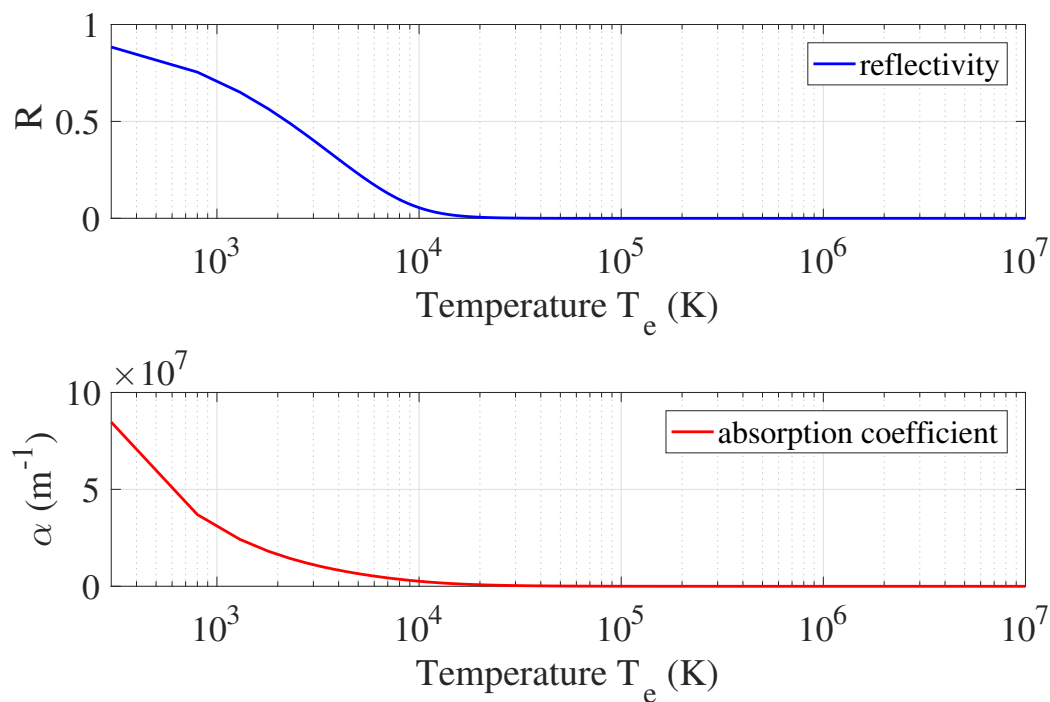


Figure 1. Reflectivity and absorption coefficient versus electron temperature. Note that the x-axis starts at 300 K.

Figure 2 shows the time evolution of the calculated electron and lattice temperatures of copper at a fluence of 10 J/cm^2 and the contour of lattice temperature versus time and position, calculated from the TTM Equations (1) and (2).

We see in Figure 2a that the lattice temperature is dramatically increased when the number of pulses increases, and it is important to mention that there is no thermal relaxation (no thermal explosion) until the last pulse, which can enhance the lattice temperature via fast thermal accumulation process. Therefore, despite laser fluence being greater than 10 J/cm^2 , the laser-plume interaction has a negligible effect during the irradiation. However, when the separation time between pulses is greater than the relaxation time, the laser-plume interaction must be taken into account. We notice also that the lattice temperature continues increasing more when the pulse number increase as well (Figure 2b). However, on the other hand, we observed immediately in Figure 2d that the lattice is more heated in the same focal volume than in Figure 2c, with some dissipation into the deeper material, for the 10th pulse's irradiation. This considerable enhancement of temperature is attributed to the heat accumulation effects, which can be called the FTAE because the separation time between pulses is less than the thermal relaxation time. Therefore, we suggest that an overheating of the same

superheated liquid was induced by the first pulse, which implies a reduction in ablation rate after each subsequent pulse. Figure 2c,d shows also that the lattice remains cold for the first few picoseconds, because the phonons carry little energy, and it takes many electron-phonon scattering processes, and therefore several picoseconds, before the electrons and the lattice reach thermal equilibrium [31].

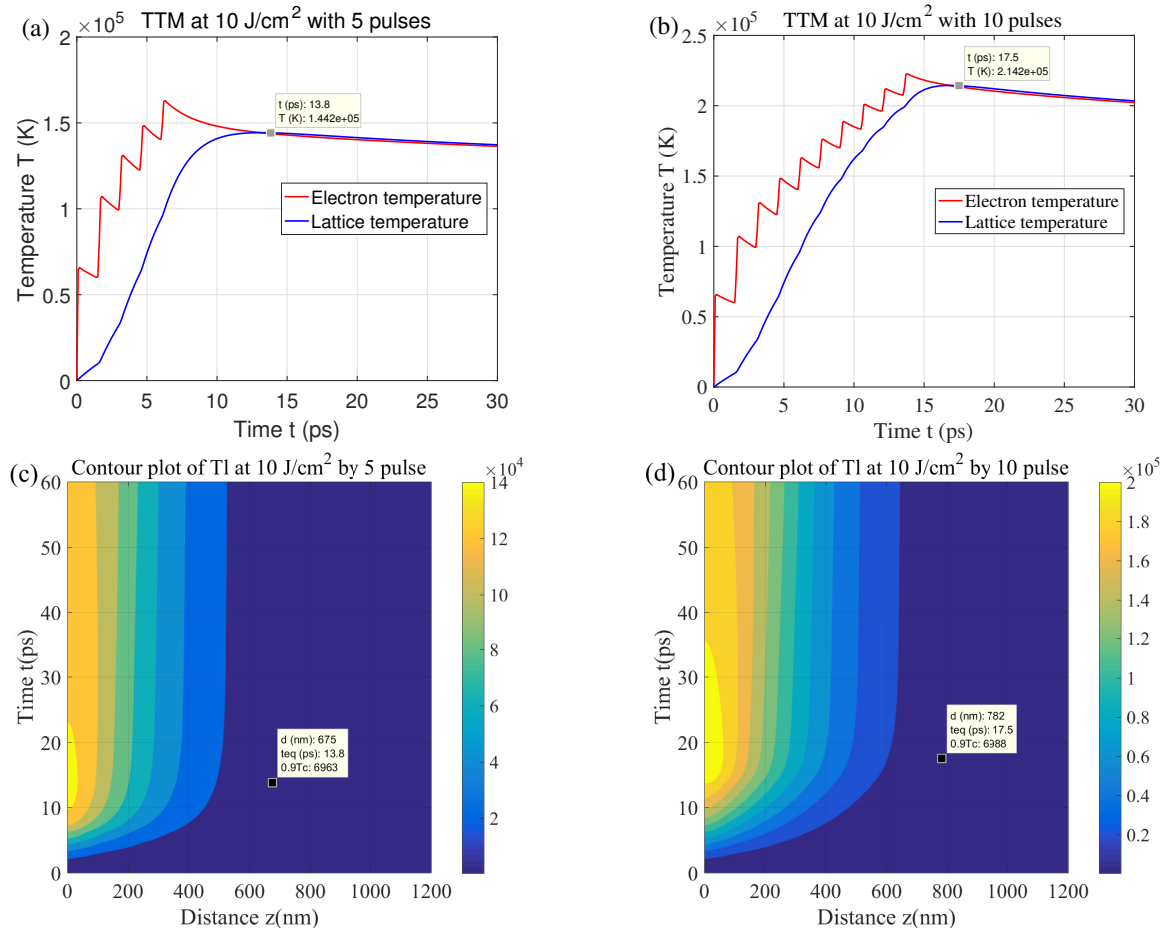


Figure 2. Evolution of electron and lattice temperature as a function of time during the irradiation by 10 J/cm²: (a) 5 pulses and (b) 10 pulses with 1.5 ps ($\frac{2}{3}$ THz) of separation time (repetition rate). Lattice temperature (T_l) versus time and position into a copper sample for an absorbed fluence of 10 J/cm²: (c) 5 pulses and (d) 10 pulses with 1.5 ps ($\frac{2}{3}$ THz) of separation time (repetition rate). d , t_{eq} and T_c represent ablation depth, time equilibrium and critical temperature, respectively. $T_c = 7696$ K. TTM: Two Temperature Model.

To understand the advantage of metal ablation by fast multipulses per burst fully, we must study all the factors that can improve the results in comparison with a single-pulse irradiation. Figure 3 shows the effect of pulse number with 1 ps (1 THz) of separation time (repetition rate) on heating the surface during irradiation. We observe that electron's temperature increases when the number of pulses increases (see Figure 3), which implies a rapid decrease in reflectivity (Figure 1). Therefore, the surface absorption can be enhanced. After each femtosecond laser pulse, the electrons transfer some of their energy to the lattice via electron-phonon collision [31], which implies a pseudo-escalation of the lattice temperature (see Figure 3); as the same remarks mentioned in [19], until the final thermal relaxation is reached. The increase in the number of pulses induces a heat accumulation, where the lattice has not had enough time to cool down after each pulse, which implies a considerable increase in the lattice temperature. Therefore, the superheated liquid temperature can be enhanced and the matter can be ejected, after phase explosion, in both vapor and drop liquid forms. We suggest that in

the multipulse regime, the vapor rate formation is higher in comparison to single-pulse irradiation, as long as the temporal separation between pulses is short enough to build up the FTAE, in contrast with the studies done in [15,22] with longer times between pulses. Therefore, this FTAE enhances the equilibrium temperature T_{eq} , but at the same time decreases the relaxation time (equilibrium time) t_{eq} , as can be seen in Figure 3, where $(T_{eq}(K), t_{eq}(s))$ are equal to $(8.97 \times 10^4, 14.1 \times 10^{-12})$, $(3.07 \times 10^4, 8.1 \times 10^{-12})$, corresponding to one and five pulses being indicated. Therefore, we suggest that, in addition to an enhancement of the superheated temperature, there is also an enhancement in vapor rate ejected with increasing number of pulses.

Following the results discussed above, we propose that a cleaner crater can be obtained at high fluences by using femtosecond laser bursts with sufficiently low interpulse separation to minimize the liquid phase during the explosion, tailoring the temporal separation between pulses.

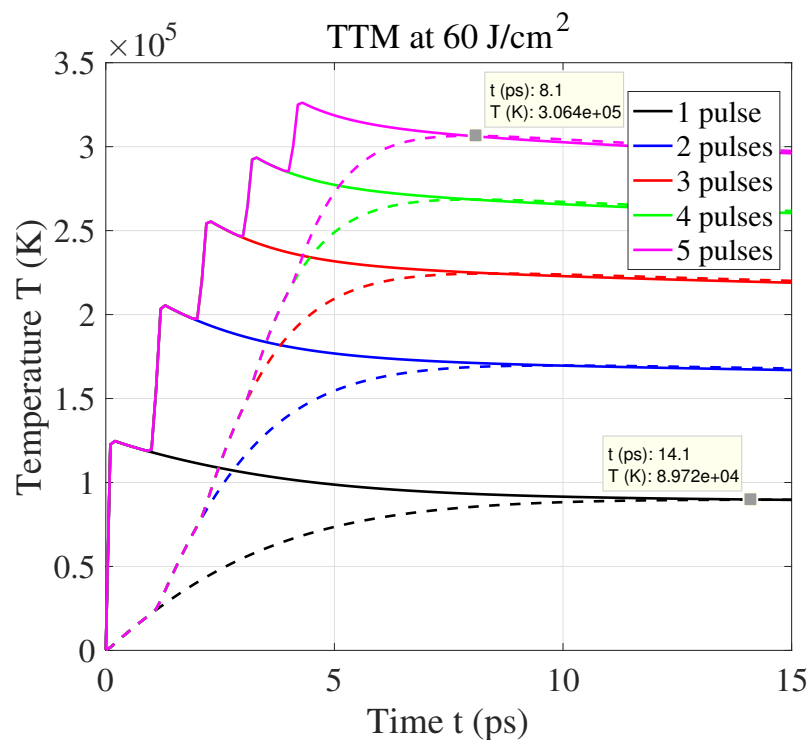


Figure 3. Time dependence of the calculated electron (solid line) and lattice (dash line) temperature with varying pulse number at a fluence of 60 J/cm^2 and 1 ps (1 THz) of separation time (repetition rate).

Figure 4 shows the effect of interpulse separation time on the thermal response of the copper surface during irradiation with four pulses per burst at 1 J/cm^2 with $t_{sep} = 0.5, 1, 1.5$ and 2 ps corresponding to $2, 1, \frac{2}{3}$ and $\frac{1}{2} \text{ THz}$ of repetition rate, respectively. It can be seen that as the interpulse separation time is decreased, the electrons reach a higher temperature, reaching a maximum at earlier times. Although the equilibrium temperature is almost the same for all four cases under study, we see that the heating rate increases when t_{sep} decreases; for example, at 5 ps, the lattice temperature corresponding to $t_{sep} = 0.5 \text{ ps}$ is nearly twice that corresponding to $t_{sep} = 2 \text{ ps}$. Therefore, we suggest that with decreasing the separation time, FTAE is more efficient.

Finally, we fix the pulse number to four and the interpulse separation time to 1 ps (1 THz repetition rate) and vary the fluence as $1, 6, 10$ and 60 J/cm^2 . Figure 5 shows the temporal behavior of the calculated electron and lattice temperatures at different laser fluences. We observe that electrons' temperature increases with increasing laser fluence, which implies that the lattice temperature increases as well via the electron-phonon collision process. Therefore, we can deduce that the ablation depth has to increase dramatically with the laser fluence.

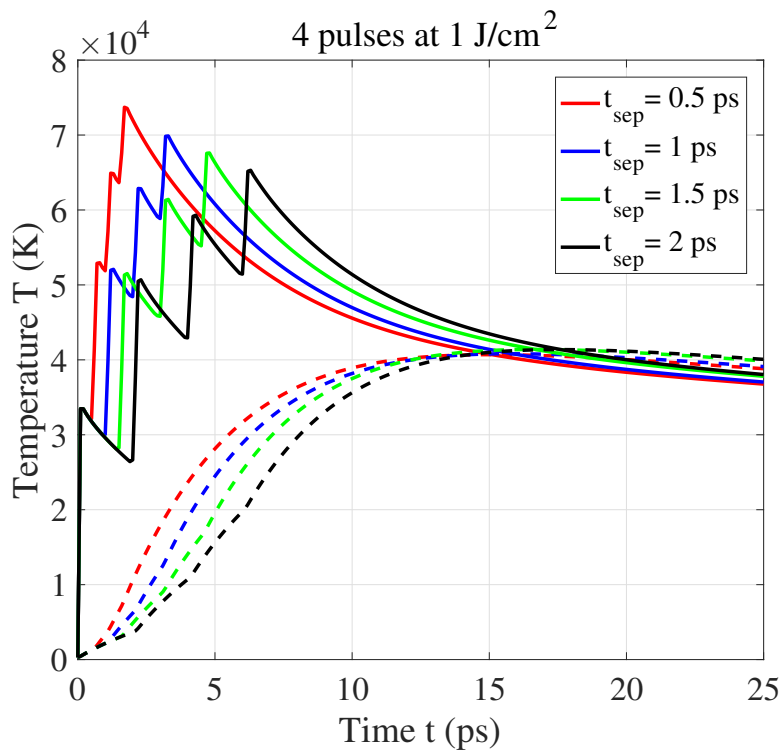


Figure 4. Time dependence of the calculated electron (solid line) and lattice (dash line) temperatures with varying separation time t_{sep} at a fluence of 1 J/cm² and four pulses.

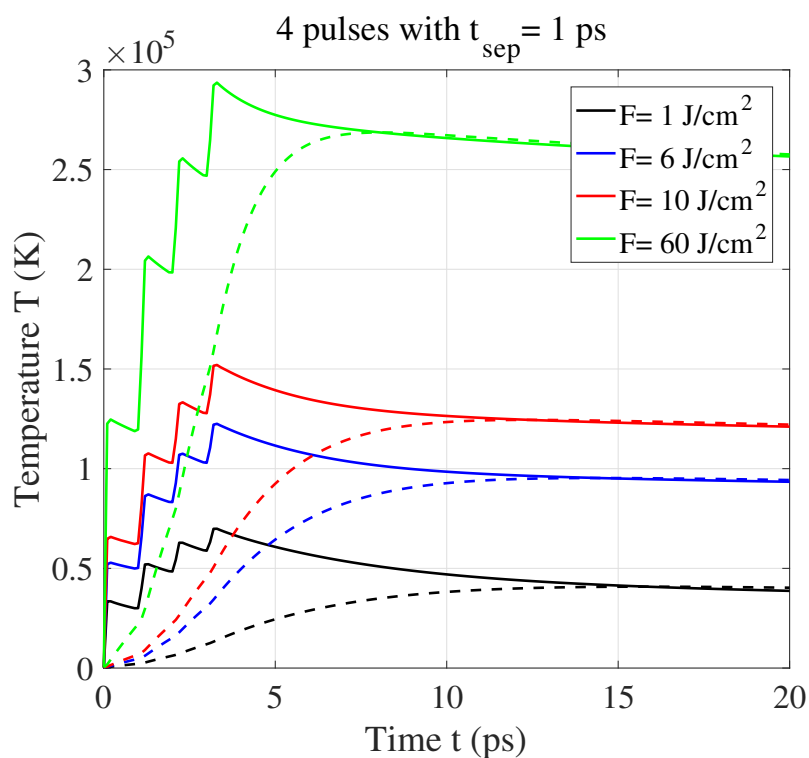


Figure 5. The time dependence of the calculated electron (solid line) and lattice (dash line) temperatures at different laser fluences with 4 pulse and 1 ps (1 THz) of separation time (repetition rate).

The proposed simulation was done to predict the ablation depths at different pulse numbers, as well as to compare our results with the experimental data at a single pulse. Figure 6 shows the theoretical ablation depth of copper irradiated by 1-, 2-, 3-, 4- and 5-fs laser pulses with a 1.5-ps ($\frac{2}{3}$ THz) separation time (repetition rate), along with experimental data from [6,11]. The ablation depth corresponding to the time equilibrium of electron-phonon relaxation t_{eq} and the condition of phase explosion $0.9 \times T_c$ are indicated in Figure 2 by a coordinate $(d, t_{eq}, 0.9 \times T_c)$. The theoretically calculated ablation depths for different pulse number are shown in (Table 1) (which correspond to the values presented in Figure 6).

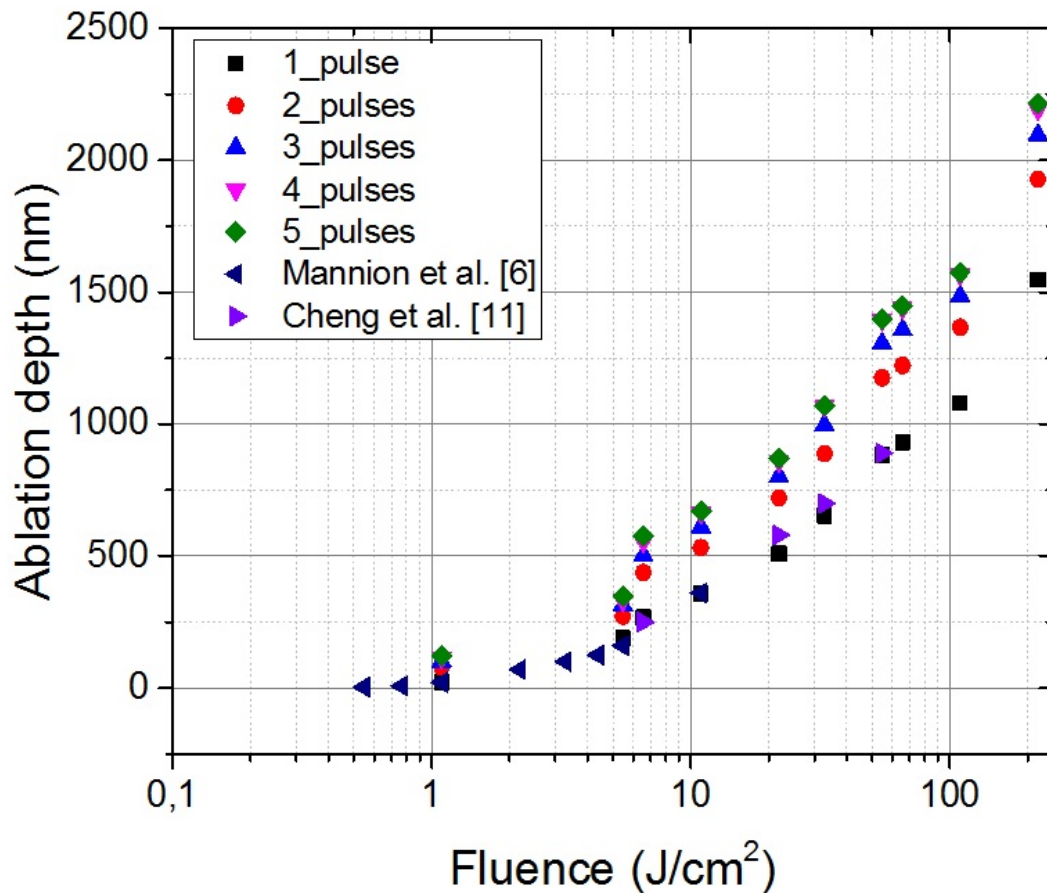


Figure 6. Simulation of ablation depth at different pulse numbers with $t_{sep} = 1.5$ ps ($\frac{2}{3}$ THz repetition rate), and experimental data for single-pulse ablation from Mannion et al. [6] and Cheng et al. [11].

Table 1. Ablation depth calculated by varying the fluence at different pulses.

Fluence (J/cm ²)	N = 1	N = 2	N = 3	N = 4	N = 5
	Ablation Depth (nm)				
1	21	78	102	116	122
5	189	272	314	332	348
6	268	438	503	556	575
10	357	532	611	664	671
20	509	720	802	861	871
30	653	888	997	1067	1070
50	883	1175	1307	1394	1398
60	931	1222	1357	1439	1447
100	1080	1367	1485	1566	1575
200	1547	1927	2096	2192	2216

Two different logarithmic dependences can be observed in Figure 6, as described in [3], which confirms the existence of two types of ablations, called gentle and strong ablations at low and high fluence [6], respectively. Figure 6 shows that the ablation depth in general is dramatically enhanced with fluence, but at the same total fluence, the rate of matter removal decreases as the number of pulses increases (see Figure 7) where ablation rate = (ablation depth (d))/(pulse number (N)). Therefore, we deduce that the most laser energy is deposited by the subsequent pulses reserved for the overheating of the same focal volume irradiated by the first pulse. We notice in Figure 7 that at $F = 1 \text{ J/cm}^2$, the ablation rate is disordered, which confirms our previous proposal [32] that the physical mechanism changes when the ablation phases change [6], where at low fluence, electron-ion collision is the most dominant, implying a gentle ablation, but at high fluence, electron-phonon collision is the most dominant, implying a strong ablation.

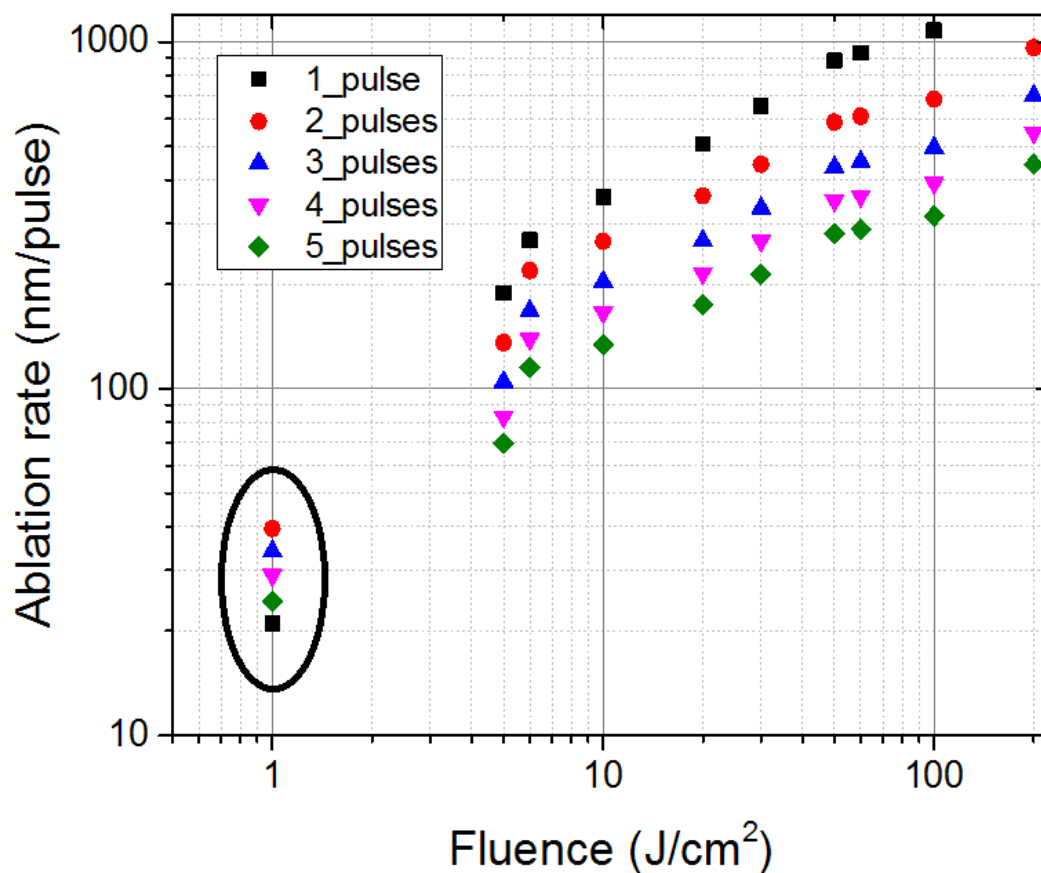


Figure 7. The ablation rate as a function of fluence at different pulse numbers with $t_{sep} = 1.5 \text{ ps}$ ($\frac{2}{3}$ THz repetition rate).

In summary, the first intense ultrashort laser pulse can produce a superheated liquid [10,13], but because the interpulse separation is less than the thermal relaxation time, the thermal wave has no time to propagate deeper into the material. This implies a thermal accumulation effect after each pulse, i.e., there will be an overheating of the same superheated liquid induced by the first pulse at the same focal volume. Then, the evaporation rate can be enhanced during the same single-phase explosion. This will produce a reduction of the liquid phase during thermal explosion, and then, a crater with high precision can be obtained at high fluence with a multipulse femtosecond laser with a fast separation time. We see also that the calculations done using this dynamic TTM are in agreement with the experimental data reported in Figure 6.

4. Conclusions

We have studied the thermal response of a copper target irradiated by a burst of femtosecond laser pulses with varying laser fluence, pulse number and interpulse separation time. This last parameter was always kept less than the thermal relaxation time. We deduce that a fast accumulation effect driven by a fast fs-laser multipulse irradiation can enhance the lattice temperature, which implies an enhancement of the mean temperature of superheated liquid at the same focal volume at a fixed total fluence, without a remarkable increase in ablation depth. Following this idea, we have proposed that by increasing the pulse number with a sufficiently low interpulse separation time, the vaporization rate can be enhanced in comparison to the melting rate during the same single-phase explosion. Thus, rapid femtosecond laser irradiation can be exploited for the cleaner and more efficient ablation of metals.

Author Contributions: Conceptualization, A.A.; Formal analysis, S.M.E.; Funding acquisition, R.R.; Methodology, A.A.; Project administration, Z.B. and E-H.A.; Software, A.A.; Supervision, Z.B. and E-H.A.; Validation, S.M.E.; Visualization, B.S., V.B. and S.M.E.; Writing-original draft, A.A.

Conflicts of Interest: The authors declare no conflict of interest.

Abbreviations

The following abbreviations are used in this manuscript:

TTM	Two Temperature Model
CE	Coulomb Explosion
FTAE	Fast Thermal Accumulation Effect
MD	Molecular Dynamics

References

- Chichkov, B.N.; Momma, C.; Nolte, S.; Von Alvensleben, F.; Tünnermann, A. Femtosecond, picosecond and nanosecond laser ablation of solids. *Appl. Phys. A* **1996**, *63*, 109–115. [[CrossRef](#)]
- Momma, C.; Nolte, S.; Chichkov, B.N.; Alvensleben, F.V.; Tünnermann, A. Precise laser ablation with ultrashort pulses. *Appl. Surf. Sci.* **1997**, *109*, 15–19. [[CrossRef](#)]
- Nolte, S.; Momma, C.; Jacobs, H.; Tünnermann, A.; Chichkov, B.N.; Wellegehausen, B.; Welling, H. Ablation of metals by ultrashort laser pulses. *JOSA B* **1997**, *14*, 2716–2722. [[CrossRef](#)]
- Leitz, K.H.; Redlingshöfer, B.; Reg, Y.; Otto, A.; Schmidt, M. Metal ablation with short and ultrashort laser pulses. *Phys. Procedia* **2011**, *12*, 230–238. [[CrossRef](#)]
- Tatra, S.; Vázquez, R.G.; Stiglbrunner, C.; Otto, A. Numerical simulation of laser ablation with short and ultra-short pulses for metals and semiconductors. *Phys. Procedia* **2016**, *83*, 1339–1346. [[CrossRef](#)]
- Mannion, P.T.; Magee, J.; Coyne, E.; O’connor, G.M.; Glynn, T.J. The effect of damage accumulation behaviour on ablation thresholds and damage morphology in ultrafast laser micro-machining of common metals in air. *Appl. Surf. Sci.* **2004**, *233*, 275–287. [[CrossRef](#)]
- Gamaly, E.G.; Rode, A.V.; Luther-Davies, B.; Tikhonchuk, V.T. Ablation of solids by femtosecond lasers: Ablation mechanism and ablation thresholds for metals and dielectrics. *Phys. Plasmas* **2002**, *9*, 949–957. [[CrossRef](#)]
- Stoian, R.; Rosenfeld, A.; Ashkenasi, D.; Hertel, I.V.; Bulgakova, N.M.; Campbell, E.E.B. Surface charging and impulsive ion ejection during ultrashort pulsed laser ablation. *Phys. Rev. Lett.* **2002**, *88*, 097603. [[CrossRef](#)] [[PubMed](#)]
- Jiang, L.; Tsai, H.L. Modeling of ultrashort laser pulse-train processing of metal thin films. *Int. J. Heat Mass Transf.* **2007**, *50*, 3461–3470. [[CrossRef](#)]
- Cheng, C.; Xu, X. Mechanisms of decomposition of metal during femtosecond laser ablation. *Phys. Rev. B* **2005**, *72*, 165415. [[CrossRef](#)]
- Cheng, C.W.; Wang, S.Y.; Chang, K.P.; Chen, J.K. Femtosecond laser ablation of copper at high laser fluence: Modeling and experimental comparison. *Appl. Surf. Sci.* **2016**, *361*, 41–48. [[CrossRef](#)]

12. Byskov-Nielsen, J.; Savolainen, J.M.; Christensen, M.S.; Balling, P. Ultra-short pulse laser ablation of copper, silver and tungsten: Experimental data and two-temperature model simulations. *Appl. Phys. A* **2011**, *103*, 447–453. [[CrossRef](#)]
13. Rethfeld, B.; Sokolowski-Tinten, K.; Von Der Linde, D.; Anisimov, S.I. Timescales in the response of materials to femtosecond laser excitation. *Appl. Phys. A* **2004**, *79*, 767–769. [[CrossRef](#)]
14. Yang, J.; Zhao, Y.; Zhu, X. Theoretical studies of ultrafast ablation of metal targets dominated by phase explosion. *Appl. Phys. A* **2007**, *89*, 571–578. [[CrossRef](#)]
15. Ren, Y.; Cheng, C.W.; Chen, J.K.; Zhang, Y.; Tzou, D.Y. Thermal ablation of metal films by femtosecond laser bursts. *Int. J. Therm. Sci.* **2013**, *70*, 32–40. [[CrossRef](#)]
16. Huang, J.; Zhang, Y.; Chen, J.K. Ultrafast solid–liquid–vapor phase change in a thin gold film irradiated by multiple femtosecond laser pulses. *Int. J. Heat Mass Transf.* **2009**, *52*, 3091–3100. [[CrossRef](#)]
17. Eaton, S.M.; Zhang, H.; Herman, P.R.; Yoshino, F.; Shah, L.; Bovatsek, J.; Arai, A.Y. Heat accumulation effects in femtosecond laser-written waveguides with variable repetition rate. *Opt. Express* **2005**, *13*, 4708–4716. [[CrossRef](#)] [[PubMed](#)]
18. Ancona, A.; Döring, S.; Jauregui, C.; Röser, F.; Limpert, J.; Nolte, S.; Tünnermann, A. Femtosecond and picosecond laser drilling of metals at high repetition rates and average powers. *Opt. Lett.* **2009**, *34*, 3304–3306. [[CrossRef](#)] [[PubMed](#)]
19. Kerse, C.; Kalaycıoğlu, H.; Elahi, P.; Çetin, B.; Kesim, D.K.; Akçaalan, Ö.; Yavaş, S.; Aşık, M.D.; Öktem, B.; Hoogland, H.; et al. Ablation-cooled material removal with ultrafast bursts of pulses. *Nature* **2016**, *537*, 84–88. [[CrossRef](#)] [[PubMed](#)]
20. Povarnitsyn, M.E.; Levashov, P.R.; Knyazev, D.V. Simulation of ultrafast bursts of subpicosecond pulses: In pursuit of efficiency. *Appl. Phys. Lett.* **2018**, *112*, 051603. [[CrossRef](#)]
21. Chowdhury, I.H.; Xu, X. Heat transfer in femtosecond laser processing of metal. *Numer. Heat Transf. Part A Appl.* **2003**, *44*, 219–232. [[CrossRef](#)]
22. Nowak, D.; Lee, M.J. Optical and Thermal Effective Masses of Copper. *Phys. Rev. B* **1972**, *5*, 2851. [[CrossRef](#)]
23. Kittel, C.; McEuen, P.; McEuen, P. *Introduction to Solid State Physics*; Wiley: New York, NY, USA, 1996; Volume 8, pp. 323–324.
24. Anisimov, S.I.; Rethfeld, B. Theory of ultrashort laser pulse interaction with a metal. In *Nonresonant Laser-Matter Interaction (NLMI-9)*; International Society for Optics and Photonics: Bellingham, WA, USA, 1997; Volume 3093, pp. 192–204.
25. Chen, J.K.; Latham, W.P.; Beraun, J.E. The role of electron-phonon coupling in ultrafast laser heating. *J. Laser Appl.* **2005**, *17*, 63–68. [[CrossRef](#)]
26. Nash, D.J.; Sambles, J.R. Surface plasmon-polariton study of the optical dielectric function of copper. *J. Mod. Opt.* **1995**, *42*, 1639–1647. [[CrossRef](#)]
27. Ren, Y.; Chen, J.K.; Zhang, Y. Optical properties and thermal response of copper films induced by ultrashort-pulsed lasers. *J. Appl. Phys.* **2011**, *110*, 113102. [[CrossRef](#)]
28. Adachi, S. *The Handbook on Optical Constants of Metals: In Tables and Figures*; World Scientific: Singapore, 2012.
29. Cheng, C.W.; Chen, J.K. Drilling of Copper Using a Dual-Pulse Femtosecond Laser. *Technologies* **2016**, *4*, 7. [[CrossRef](#)]
30. Kotsedi, L.; Kaviyarasu, K.; Fuku, X.G.; Eaton, S.M.; Amara, E.H.; Bireche, F.; Ramponi, R.; Maaza, M. Two temperature approach to femtosecond laser oxidation of molybdenum and morphological study. *Appl. Surf. Sci.* **2017**, *421*, 213–219. [[CrossRef](#)]
31. Sundaram, S.K.; Mazur, E. Inducing and probing non-thermal transitions in semiconductors using femtosecond laser pulses. *Nat. Mater.* **2002**, *1*, 217–224. [[CrossRef](#)] [[PubMed](#)]
32. Abdelmalek, A.; Bedrane, Z.; Amara, E.H. Thermal and non-thermal explosion in metals ablation by femtosecond laser pulse: Classical approach of the Two Temperature Model. *J. Phys. Conf. Ser.* **2018**, *987*, 012012. [[CrossRef](#)]

